

STSyn: Speeding Up Local SGD with Straggler-Tolerant Synchronization

Feng Zhu, Jingjing Zhang, *Member, IEEE* and Xin Wang, *Senior Member, IEEE*

arXiv:2210.03521v2 [cs.LG] 26 Oct 2022

Abstract—Synchronous local stochastic gradient descent (local SGD) suffers from some workers being idle and random delays due to slow and straggling workers, as it waits for the workers to complete the same amount of local updates. In this paper, to mitigate stragglers and improve communication efficiency, a novel local SGD strategy, named STSyn, is developed. The key point is to wait for the K fastest workers, while keeping all the workers computing continually at each synchronization round, and making full use of any effective (completed) local update of each worker regardless of stragglers. An analysis of the average wall-clock time, average number of local updates and average number of uploading workers per round is provided to gauge the performance of STSyn. The convergence of STSyn is also rigorously established even when the objective function is nonconvex. Experimental results show the superiority of the proposed STSyn against state-of-the-art schemes through utilization of the straggler-tolerant technique and additional effective local updates at each worker, and the influence of system parameters is studied. By waiting for faster workers and allowing heterogeneous synchronization with different numbers of local updates across workers, STSyn provides substantial improvements both in time and communication efficiency.

Index Terms—Local SGD, heterogeneous synchronization, straggler tolerance, distributed learning

I. INTRODUCTION

As the size of datasets increases exponentially, it is no longer economic and feasible to leverage all the data to update the model parameters in large-scale machine learning, which magnifies the disadvantage of gradient descent (GD) methods in computational complexity. Instead, stochastic gradient descent (SGD) that uses just one or a mini-batch of samples is proved to converge faster and can achieve significantly reduced computation load [1]–[3]. Therefore, SGD has become the backbone of large-scale machine learning tasks.

To exploit parallelism and further accelerate the training process, the distributed implementation of worker nodes, i.e., distributed learning, has been gaining popularity [4]–[6]. The parameter server (PS) setting is one of the most common scenarios of SGD-based distributed learning frameworks, where in each iteration the PS aggregates the uploaded gradients/models from all the worker nodes to update the global parameter [2], [4], [5], [7]–[9]. In such a setting,

The authors are with the Key Laboratory for Information Science of Electromagnetic Waves (MoE), Department of Communication Science and Engineering, School of Information Science and Technology, Fudan University, Shanghai 200433, China (e-mail: \{20210720072, jingjingzhang, xwang11\}@fudan.edu.cn). (Corresponding author: Jingjing Zhang.)

This work was supported by the National Natural Science Foundation of China Grants No. 62101134 and No. 62071126, and the Innovation Program of Shanghai Municipal Science and Technology Commission Grant 20JC1416400.

communication cost has become the bottleneck for the performance of the system due to the two-way communication and the larger number of parameters to be updated at each iteration [1], [5], [10]–[12]. Accordingly, a novel scheme justified by the name local SGD is proposed to reduce the communication frequency between the PS and the workers by allowing each worker to perform local updates.

The idea of local SGD is first introduced in [6] where each worker performs a certain number of local updates instead of one, and the PS aggregates the latest model of each worker as the final output. However, the scheme in [6] has been proved to be no better than single-worker algorithms in the worst-case scenario due to the divergence of local optima across workers [13]. To address this issue, [14] proposes the federated averaging (FedAvg) scheme, where each sampled worker runs multiple local updates before uploading the local model to the central server for aggregation and then the server re-sends the aggregated model back to the workers to repeat the above process. By increasing the communication frequency, FedAvg has been proved to be communication-efficient and enjoy remarkable performance under homogenous data distribution. The convergence analysis of the latter is widely explored in [15]–[18]. It should also be pointed out that FedAvg is proved to be able to achieve linear speedup concerning the number of workers in this setting. Furthermore, when data is heterogeneously distributed, the convergence of FedAvg is also proved by [19]–[23], yet the linear speedup is no longer accessible since the convergence rate depends weakly on the number of workers. Local SGD has also been proved to achieve better time and communication performance than large mini-batch training with the size of the mini-batch being the same as the total batchsize used in a training round of local SGD [24]. The heterogeneous synchronization of local SGD under heterogeneous data distribution is also studied in [25], [26]. [25] proposes the FedNova algorithm to balance the heterogeneity of the number of local updates across workers; while [26] studies the impact of data heterogeneity on heterogeneous synchronization.

Adaptive Communication Strategies for Local SGD: It has been proved by [15], [21] that it is theoretically reasonable and advantageous to vary the communication frequency as the training proceeds. The authors of [27] present the convergence analysis of periodic averaging SGD (PASGD), which is FedAvg with no user sampling, and propose an adaptive scheme that gradually decreases the communication frequency between workers and the server to reduce total communication rounds. Meanwhile, [28] also proposes an adaptive strategy based on PASGD where the communication

frequency is increased along the training process to achieve a decrease in the true convergence time. In addition, [29] proposes the STagewise Local SGD (STL-SGD) that increases the communication period along with decreasing learning rate to achieve further improvement.

Local SGD presents a possibility to reduce the communication cost of the system; yet, other than communication efficiency, the wall-clock time required for convergence is also an important issue. As the consequence of the discrepancy in worker nodes, there is considerable variability in the computing time of different machines, and the machines that consume excessively more time per round than others are normally known as stragglers [30]. Numerous researches have been conducted in the development of straggler-tolerant techniques, which can be generally categorized into synchronous schemes and asynchronous ones.

Dealing with Straggling in Synchronous SGD Schemes: In synchronous parallel SGD, the PS always waits for all the workers to finish their computation. As a result, the whole process could be severely slowed down due to the existence of potential stragglers. One way to mitigate the effect of straggling is to exploit redundancy such as [31]–[35] that allow the PS to wait for only a subset of workers by utilizing storage and computation redundancy. Other than redundancy, [36] develops the FlexRR system that attempts to detect and avoid stragglers. Another well-known truth is that the convergence analysis of M -worker synchronous parallel SGD is the same as mini-batch SGD, only with the mini-batch size enlarged M times. Inspired by this idea, [9] and [37] propose the K -sync SGD where the PS only waits for the first K workers to finish their computation. In addition, [37] extends the K -sync SGD to K -batch-sync SGD in which the PS updates the parameter using the first K mini-batches that finish, such that no worker is idle in each training round.

Dealing with Stragglers with Asynchronous SGD: Apart from confronting stragglers in the synchronous schemes, asynchronous SGD (ASGD) is also proposed to address this issue [38]. In ASGD, the PS updates the parameter immediately after any worker finishes its computation and uploads it to the server. Apparently, the time used per round of ASGD schemes is much less than that used in synchronous SGD. Nevertheless, since the gradient used to update the parameter may not be the one used to compute it, the trade-off between wall-clock time and the staleness of the gradient becomes the main issue in ASGD, for which a number of variants of ASGD have been proposed. In [39], the authors develop the Hogwild! scheme which is a lock-free implementation of ASGD and proves its effectiveness both theoretically and experimentally; and [40] improves the performance of ASGD based on Hogwild! with no conflict in parallel execution. In [37], the authors review the K -async SGD and K -batch-async SGD first introduced in [9] and [41] respectively, and propose the AdaSync scheme to achieve the best error-runtime trade-off. Another trend of research is to process the delayed gradients in ASGD. To this end, [42] proposes the AdaDelay algorithm that imposes a penalty on delayed gradients, and [43] introduces the DC-ASGD scheme that compensates for the delayed gradients to make full use of all the gradients.

A. Our Contributions

This paper develops a novel local SGD scheme, named STSyn, with heterogeneous synchronization under homogeneous data distribution in a distributed PS architecture that enables straggler mitigation. The main contributions of our work are summarized as follows:

- We propose a novel local SGD scheme that allows different numbers of local updates across workers with robustness to stragglers. Although quite some local SGD variants with heterogeneous synchronization have been proposed previously, to the best of our knowledge, this is the first work to capitalize on heterogeneous synchronization to speed up local SGD under homogenous data distribution.
- We provide the analysis of the average runtime, average number of uploading workers and average number of local updates per round, to justify the improvement of STSyn in time and communication efficiency. We also analytically establish the convergence of STSyn and prove that it can achieve a sublinear convergence rate of $\mathcal{O}(1/J)$ as other local SGD variants, yet with a reduced convergence upper bound.
- Finally, we present experiment results to corroborate the superiority of STSyn against state-of-the-art schemes in terms of wall-clock time and communication efficiency for independently and identically distributed (i.i.d.) data. The influence of the system hyper-parameters is also studied.

The rest of the paper is organized as follows. Section II describes the system model. Development of the proposed STSyn scheme is delineated in Section III. Section IV presents the analysis of STSyn. Numerical results are provided in Section V. Section VI concludes the work.

Notations: Boldface lowercase letters and calligraphic letters represent vectors and sets, respectively; \mathbb{R} denotes the real number fields; $\mathbb{E}[\cdot]$ denotes the statistical expectation; \cup denotes the union of sets; $\mathcal{A} \subseteq \mathcal{B}$ means that set \mathcal{A} is a subset of set \mathcal{B} ; $|\mathcal{A}|$ denotes the number of elements in set \mathcal{A} ; ∇F represents the gradient of function F ; $\|\mathbf{x}\|$ denotes the ℓ_2 -norm of vector \mathbf{x} ; $\langle \mathbf{x}, \mathbf{y} \rangle$ denotes the inner product of vectors \mathbf{x} and \mathbf{y} .

II. PROBLEM FORMULATION

A. System Model

We first introduce the general problem framework of distributed SGD with local updates in order to reduce communication overhead. Our objective is to minimize the following empirical risk function given as

$$F(\mathbf{w}) = \frac{1}{N} \sum_{i=1}^N f(\mathbf{w}; \xi_i), \quad (1)$$

where variable $\mathbf{w} \in \mathbb{R}^d$ is the d -dimensional parameter to be optimized; N is the total number of samples in dataset $\mathcal{D} = \{\xi_i\}_{i=1}^N$; and $f(\mathbf{w}; \xi_i)$ is a certain loss function that depends on parameter \mathbf{w} and sample ξ_i from dataset \mathcal{D} .

To implement the local-SGD-based training process, a parameter server setting with M workers, denoted by set $\mathcal{M} \triangleq \{1, \dots, M\}$, is considered. Each worker m maintains a local dataset \mathcal{D}_m , which is equally and homogeneously allocated from the global training dataset, and we have $\mathcal{D} = \bigcup_{m \in \mathcal{M}} \mathcal{D}_m$. To elaborate on the communication and updating protocol, we define \mathbf{w}^j as the global parameter, and $\mathbf{w}_m^{j,0}$ as the local parameter that worker $m \in \mathcal{M}$ has available at training round j prior to computation.

In local SGD, at each synchronization round j , the PS first broadcasts the global model parameter \mathbf{w}^j to a subset of workers $\mathcal{M}^j \subseteq \mathcal{M}$. Then by setting the local model as $\mathbf{w}_m^{j,0} = \mathbf{w}^j$, each worker m in \mathcal{M}^j starts to perform local updates. At the end of round j , each worker m is assumed to complete $U_m^j \geq 0$ local updates, with each given as

$$\mathbf{w}_m^{j,u+1} = \mathbf{w}_m^{j,u} - \frac{\alpha}{B} \sum_{b=1}^B \nabla F(\mathbf{w}_m^{j,u}; \xi_{m,b}^{j,u}), \quad (2)$$

for any $u = 0, \dots, U_m^j - 1$ if $U_m^j \geq 1$. Here α is the stepsize; the mini-batch $\{\xi_{m,b}^{j,u}\}_{b=1}^B$ of size B is generated randomly for each local update from dataset \mathcal{D}_m ; and $\nabla F(\mathbf{w}_m^{j,u}; \xi_{m,b}^{j,u})$ is the local gradient of loss function F computed with local parameter $\mathbf{w}_m^{j,u}$ and data sample $\xi_{m,b}^{j,u}$. After the computation, the PS then selects a subset $\mathcal{S}^j \subseteq \mathcal{M}^j$ of S^j workers to upload their local parameters, yielding the global parameter \mathbf{w}^{j+1} given as

$$\mathbf{w}^{j+1} = \frac{1}{S^j} \sum_{m \in \mathcal{S}^j} \mathbf{w}_m^{j,U_m^j}. \quad (3)$$

The next round $j+1$ then starts and the training continues until a convergence criterion is satisfied, with the total number of rounds defined as J . The whole process is illustrated in Fig. 1.

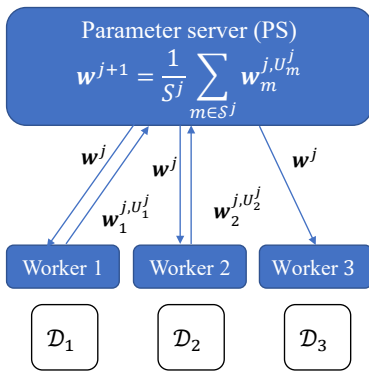


Fig. 1. Illustration of the PS setting with $M = 3$, $\mathcal{M}^j = \{1, 2, 3\}$ and $\mathcal{S}^j = \{1, 2\}$.

B. Preliminaries

Based on the distributed PS architecture under consideration, our proposed scheme stems from a couple of local SGD variants, which we briefly review next.

Federated Averaging (FedAvg). One pioneering work on local update is the so-called FedAvg. More precisely, at each round, the PS first randomly selects a subset $\mathcal{M}^j \subseteq \mathcal{M}$ of workers to broadcast the global parameter to. Then each selected worker m performs the same amount $U_m^j = U$ of local updates and sends the local parameter back to the PS, i.e., we have $\mathcal{S}^j = \mathcal{M}^j$. In particular, when all the workers participate in the computation in each round, i.e., with $\mathcal{S}^j = \mathcal{M}^j = \mathcal{M}$, we can arrive at periodic-averaging SGD (PASGD) [27].

Adaptive Communication Strategy (AdaComm). Building upon PASGD, [28] proposes an adaptive communication strategy called AdaComm in order to achieve a faster convergence speed in terms of wall-clock runtime. This is achieved by adaptively increasing the communication frequency between the PS and the workers. Note here that each worker still performs the same number of local updates in each training round.

Apart from aforementioned local SGD variants, we also review an asynchronous-based scheme with straggler mitigation, which will be used for comparison to demonstrate the superiority of our scheme in wall-clock time.

Adaptive Synchronization (AdaSync). An asynchronous scheme, named AdaSync, is introduced in [37] to perform distributed learning in an asynchronous manner over different time intervals. Moreover, by adaptively selecting the number of workers to wait for in each interval, AdaSync can achieve a more desirable error-runtime trade-off as compared to fully-synchronous and fully-asynchronous schemes.

C. Performance Metrics

In addition to training/learning accuracy, the time consumption and communication cost with the distributed learning scheme are also important performance metrics. Indeed, the training accuracy should be evaluated as a function of time and/or communication cost to fairly gauge the time/communication efficiency of a learning scheme. To this end, we specifically define wall-clock runtime and the communication cost as follows.

Firstly, the wall-clock runtime for each worker m at the local iteration u ($u < U_m^j$) of round j is defined as the time elapsed while computing the mini-batch gradient $\frac{1}{B} \sum_{b=1}^B \nabla F(\mathbf{w}_m^{j,u}; \xi_{m,b}^{j,u})$. It is denoted by $T_m^{j,u}$, and is assumed to conform to exponential distribution with mean μ . We also assume that the random variable $T_m^{j,u}$ is independent across all workers, rounds and local iterations. Therefore, the total time consumed at round j can be written as

$$T^j = \max_{m \in \mathcal{S}^j} \left\{ \sum_{u=0}^{U_m^j-1} T_m^{j,u} \right\}. \quad (4)$$

Secondly, notice that the global model parameter broadcast from the PS to workers and the local parameters sent from the workers to the PS, are of the same size. Hence, at each synchronization round j , we can simply define the communication cost C^j as the sum of the number $|\mathcal{M}^j|$ of workers that

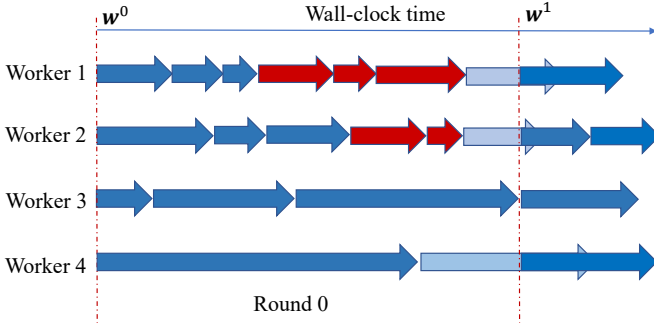


Fig. 2. Illustration of STSyn with $M = 4$, $U = 3$ and $K = 3$. In round 0, worker 1, 2 and 3 are the fastest $K = 3$ workers that have completed $U = 3$ local updates; the red arrows represent the additional local updates performed by the fastest $K - 1 = 2$ workers; and the arrows in light blue represent the straggling updates that are cancelled.

download the global model from the PS, and the number $|\mathcal{S}^j|$ of workers that send the local update to the PS; i.e.,

$$C^j = |\mathcal{M}^j| + |\mathcal{S}^j|. \quad (5)$$

These two performance metrics will be studied in the theoretical analysis in Section IV and will be used to evaluate the time/communication efficiency of the schemes in the experimental results in Section V.

III. LOCAL SGD WITH HETEROGENEOUS SYNCHRONIZATION (STS^N)

In this section, we develop a novel strategy, named STSyn, which aims at speeding up local SGD under i.i.d. data with heterogeneous synchronization. The key points are two-fold: First, in each training round, no worker stops computing until the K th fastest one completes U local updates. Hence, the faster the worker is, the more local updates it computes. As compared to the typical local SGD where only the selected workers carry out the same amount of local updates in each training round, no worker in STSyn suffers from being idle. As a result, STSyn takes the advantage of both straggler mitigation and training speedup. Second, in the aggregation phase, any worker that finishes at least one local update, i.e., with $U_m^j \geq 1$, sends its local parameter back to the PS. By increasing the number of workers that participate in the aggregation with each effective local update, STSyn can further accelerate the training process. This also brings the benefit of communication efficiency in the sense that the reduction of synchronization rounds can compensate the increase of communication cost at each round.

Building on these ideas, we propose the novel STSyn scheme as follows. In particular, at each training round j , the PS sends the current global model parameter \mathbf{w}^j to all the workers in \mathcal{M} , i.e., we have $\mathcal{M}^j = \mathcal{M}$. Then each worker m sets its local model parameter $\mathbf{w}_m^{j,0} = \mathbf{w}^j$ and begins its computation. After computing the first U local updates, each worker acknowledges the completion but continues to update locally. Once the PS receives K ($K \leq M$) acknowledgments, it terminates the computation of round j . However, for the rest $M - K$ straggling workers, they might have finished at

Algorithm 1 STSyn

Input: number of workers M , constant U, K , stepsize $\alpha > 0$, batch size B

Server executes:

Initiate \mathbf{w}^0

for $j = 0, 1, \dots, J - 1$ **do**

Sends the global model \mathbf{w}^j to all the workers in \mathcal{M}

for each worker $m \in \mathcal{M}$ **do**

Executes $\text{WorkerUpdate}(m, \mathbf{w}^j)$

end for

if receives K acknowledgements **then**

Stops the computation of the round and collects the

local models $\{\mathbf{w}_m^{j, U_m^j}\}_{m \in \mathcal{S}^j}$

end if

Updates \mathbf{w}^j with (3)

end for

WorkerUpdate(m, \mathbf{w}^j):

Sets local model $\mathbf{w}_m^{j,0} = \mathbf{w}^j$ and $U_m^j = 0$

repeat

Updates its local model via (2) and sets $U_m^j = U_m^j + 1$

if $U_m^j == U$ **then**

Sends an acknowledgment to the server

end if

stops computing immediately when noticed (by the server)
the end of current round

if $U_m^j \geq 1$ **then**

$\mathcal{S}^j \ni m$

Uploads its latest model \mathbf{w}_m^{j, U_m^j} to the server

end if

least one local update, i.e., with $U_m^j \geq 1$, which can also be used for the global update. In other words, at round j , we might have a subset $\mathcal{S}^j \subseteq \mathcal{M}$ with $S^j \geq K$ workers that have completed at least one update.

At the end of training round j , each worker in the subset \mathcal{S}^j (instead of the set of the fastest K workers) is required to upload its latest model parameter \mathbf{w}_m^{j, U_m^j} . Then, the PS updates the global parameter \mathbf{w}^j through (3). The next round $j+1$ starts similarly and the training continues. An illustration of the STSyn scheme is shown in Fig. 2. Note that the cost and time elapsed of communicating the acknowledgment are assumed negligible here as they are typically much smaller than those with the local parameters. The complete procedure of STSyn is summarized in Algorithm 1.

Merits of STSyn: To the best of our knowledge, this is the first work to capitalize on heterogeneous synchronization to speed up local SGD. The compound of the additional local updates from both the fastest K workers and the rest $M - K$ stragglers brings multiplicative benefits; consequently, STSyn can outperform both the synchronous and asynchronous SGD schemes. Intuitively, compared to the synchronous schemes such as FedAvg, with the choice $U_m^j = U$ and $\mathcal{M}^j = \mathcal{M}$, STSyn collects more local updates in a training round and also only has to wait for the fastest K workers, thereby achieving better time and communication efficiency. For K -

async SGD, it is well known that it is competitive in terms of wall-clock time by utilizing stale gradients. However, STSyn can be even superior by cancelling the super slow local updates of the stragglers that are unfinished at each synchronization round, which indeed has limited contribution. In a nutshell, the straggler-tolerant techniques and the extra effective local updates together endow STSyn with the advantages both in wall-clock time and communication efficiency over state-of-the-art schemes.

IV. PERFORMANCE ANALYSIS

In this section, we provide the analysis of the average runtime, average number of local updates and average number of uploading workers for each training round along with numerical illustrations. The benefits from additional effective local updates from the K fastest workers and the rest $M - K$ stragglers are highlighted via comparison with FedAvg. In addition, convergence of the proposed STSyn is rigorously established.

A. Average Wall-Clock Runtime

As specified in Subsection II-C, we assume that the wall-clock times $\{T_m^{j,u}\}$ are i.i.d. exponential random variables across workers, rounds and local iterations, i.e., we have $T_m^{j,u} \sim \text{Exp}(\mu)$.

At each round j , to carry out $U_m^j = U$ local updates, the runtime T_m^j of each worker m is given as $T_m^j := \sum_{u=0}^{U-1} T_m^{j,u}$. It then readily follows that T_m^j is an Erlang random variable with mean $U\mu$ and variance $U\mu^2$. Since the PS only waits for the K th fastest worker to finish U local updates, the average wall-clock time \bar{T} taken per round can be computed as

$$\bar{T} = \mathbb{E}[T_{K:M}^j] = \frac{\mu M!}{(K-1)!(M-K)!} I \quad (6)$$

where $T_{K:M}^j$ is the K th order statistic of variables $\{T_m^j\}_{m \in \mathcal{M}}$, as analyzed in [44], and we have the integral

$$I = \int_0^\infty x \{Q(x)\}^{K-1} \{1 - Q(x)\}^{M-K} q(x) dx, \quad (7)$$

with $q(x)$ and $Q(x)$ being the functions

$$q(x) = \frac{x^{U-1} \exp(-x/\mu)}{\mu^U (U-1)!},$$

$$Q(x) = \frac{\int_0^x t^{U-1} \exp(-t) dt}{(U-1)!}.$$

B. Average Number of Local Updates and Uploading Workers

Average Number of Local Updates per Round. It is known that the average runtime per round is $\mathbb{E}[T_{K:M}^j]$ and we have $T_m^{j,u} \sim \text{Exp}(\mu)$. As a result, the average number \bar{U} of local updates that each worker m performs can be derived as

$$\bar{U} = \mathbb{E}[U_m^j] = \frac{\mathbb{E}[T_{K:M}^j]}{\mu} = \frac{M!}{(K-1)!(M-K)!} I. \quad (8)$$

It is easy to see that \bar{U} increases as K since $\mathbb{E}[T_{K:M}^j]$ does. On one hand, a larger K indicates more local updates at each

worker, which are beneficial for communication efficiency. On the other hand, the robustness against stragglers is decreased as we need to wait for more workers. Therefore, a trade-off between communication and time efficiency should be addressed, which is further explored through experiments in Section V.

Average Number of Uploading Workers per Round. Note that in STSyn, any worker that can finish at least one local update sends back its completed local parameter. To elaborate, for any integer $s \leq M$, we define as $T_{s:M}^{j,0}$ the s th order statistic of i.i.d. variables $\{T_m^j\}_{m=1}^M$, where T_m^j is the runtime of worker m consumed for the first local update. Then within runtime $T_{K:M}^j$ at round j , the number of selected workers S^j can be given as

$$S^j = \max \left\{ s \mid T_{s:M}^{j,0} \leq T_{K:M}^j \right\}. \quad (9)$$

For exponential distribution, the average of $T_{s:M}^{j,0}$ can be approximated as [37],

$$\mathbb{E}[T_{s:M}^{j,0}] = \sum_{i=M-s+1}^M \frac{\mu}{i} \approx \mu \log \frac{M}{M-s}. \quad (10)$$

By using (10) and (9), $\mathbb{E}[S^j]$ can be derived as

$$\mathbb{E}[S^j] \approx M - \exp \left(\log M - \frac{M!}{(K-1)!(M-K)!} I \right). \quad (11)$$

It is easy to see that $\mathbb{E}[S^j]$ is also positively related to K and U . That is to say, as the PS waits for more workers to finish more local iterations, a larger number of workers could complete at least one update and be selected to upload their local parameters at each round.

Fig. 3 shows an example of a certain training round of STSyn with $M = 40$, $K = 30$, and $U = 2$. It can be observed that almost half of the workers have completed more than $U = 2$ local updates and 7 stragglers have one. These additional local updates are beneficial to the convergence speed, as will be illustrated in the sequel. Over 200 rounds, we also calculate the average number of local updates and that of workers selected to upload per round. As indicated in Fig. 3, the values are 2.63 and 37.155, both of them are consistent with the derived results $\mathbb{E}[U_m^j] = 2.6352$ and $\mathbb{E}[S^j] = 37.132$ in (8) and (11), respectively.

Benefits from Additional Effective Local Updates. By keeping all the workers computing until the end of each round, STSyn makes full use of any completed (effective) local update. This includes the additional ones performed both by the fastest K workers and by the rest $M - K$ stragglers (see Fig. 3), as compared to the typical local SGD methods such as FedAvg with $U_m^j = U$. The respective benefits of exploring both types are illustrated in Fig. 4. In particular, STSyn_modified1 merely utilizes the additional local updates of the fastest workers, i.e., we have $U_m^j \geq U$ for the K fastest workers and $S^j = K$; while STSyn_modified2 only keeps the additional ones performed by the stragglers, i.e., we have $U_m^j = U$ for the K fastest workers and $S^j \geq K$. It can be observed that both of STSyn_modified1 and STSyn_modified2 require fewer training rounds than the baseline FedAvg to reach the same test accuracy. In other words, any type of

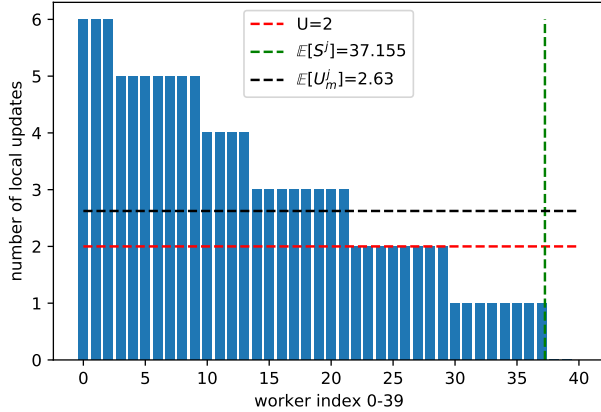


Fig. 3. The numbers of local updates across workers in a training round with $M = 40$, $K = 30$ and $U = 2$.

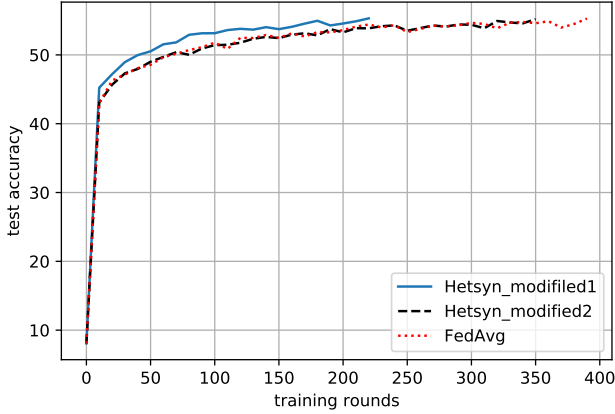


Fig. 4. Illustration of the impact of additional effective local updates on learning accuracy. In contrast to STSyn, STSyn_modified1 is fixed with $S^j = K$; and STSyn_modified2 is fixed with $U_m^j = U$.

effective local update is favorable. It is also evidently seen that the ones of the fastest workers are indeed more useful. Furthermore, the joint effect of the two types is magnificent, which will be shown in Section V.

C. Convergence Analysis

We next rigorously establish the convergence of STSyn. Our convergence analysis is based on the following standard assumptions, which are widely adopted in e.g., [16], [19], [23].

Assumption 1 (Unbiasedness and Variance Boundedness)
For fixed model parameter vector \mathbf{w} , the stochastic gradient $\nabla F(\mathbf{w}; \xi)$ is an unbiased estimator of the true gradient $\nabla F(\mathbf{w})$, i.e., we have

$$\mathbb{E}_\xi[\nabla F(\mathbf{w}; \xi)] = \nabla F(\mathbf{w}). \quad (12)$$

Moreover, there exists a scalar C such that

$$\mathbb{E}_\xi \left[\|\nabla F(\mathbf{w}; \xi) - \nabla F(\mathbf{w})\|^2 \right] \leq C. \quad (13)$$

Assumption 2 (Smoothness and Lower Boundedness) *The objective function F is L -smooth, i.e.,*

$$\|\nabla F(\mathbf{w}_1) - \nabla F(\mathbf{w}_2)\| \leq L \|\mathbf{w}_1 - \mathbf{w}_2\|, \quad (14)$$

$$F(\mathbf{w}_1) - F(\mathbf{w}_2) \leq \langle \nabla F(\mathbf{w}_2), \mathbf{w}_1 - \mathbf{w}_2 \rangle + \frac{L}{2} \|\mathbf{w}_1 - \mathbf{w}_2\|^2, \quad (15)$$

$\forall \mathbf{w}_1, \mathbf{w}_2 \in \mathbb{R}^d$. We also assume that the objective function F is bounded below by a scalar F^* .

Based on these assumptions, we can then derive an upper bound for the expectation of the average squared gradient norms $\frac{1}{J} \mathbb{E} \left[\sum_{j=0}^{J-1} \|\nabla F(\mathbf{w}^j)\|^2 \right]$ of the objective function F , which is a common metric used for convergence analysis with general nonconvex objectives. Before that, we need the following lemma.

Lemma 1: *For each worker m , suppose that STSyn with a fixed stepsize α satisfies the inequalities*

$$\frac{L^2 \alpha^2 (U_m^j + 1)(U_m^j - 2)}{2} + L \alpha U_m^j \leq 1 \quad \forall m, j,$$

and $1 - \delta \geq L^2 \alpha^2$, (16)

with some constant $\delta \in (0, 1)$. Then the expectation of the one-step difference of the objective function F can be upper bounded by

$$\begin{aligned} \mathbb{E} [F(\mathbf{w}^{j+1}) - F(\mathbf{w}^j)] &\leq \sum_{s \in S^j} \frac{-(U_m^j - 1 + \delta)\alpha}{2S^j} \|\nabla F(\mathbf{w}^j)\|^2 \\ &+ \frac{1}{S^j} \sum_{m \in S^j} \frac{L \alpha^2 U_m^j C}{2B} \left(U_m^j + \frac{L(2U_m^j - 1)(U_m^j - 1)\alpha}{6} \right). \end{aligned} \quad (17)$$

Proof. The proof is presented in Appendix A. □

Lemma 1 provides the expectation of the one-step difference of the objective function F . From the right-hand side (RHS) of (17), we can observe that, the first term caused by the gradient $\nabla F(\mathbf{w}^j)$ decreases as U_m^j grows larger. On the other hand, the second term, which is the noise term introduced by the stochasticity of the gradients, is positively related with U_m^j . By selecting a reasonable value of U , we are able to achieve a balance between the one-step descent and the variance in STSyn. Furthermore, by involving the stragglers with $U_m^j \in [1, U]$ to upload along with the fastest workers with $U_m^j \geq U$, the noise term becomes depressed by averaging, revealing the effectiveness of additional local updates, as shown in Fig. 4.

Directly from Lemma 1, we can obtain Corollary 1 by i) bounding $U_m^j \leq U_0$, with U_0 being some constant, as the possibility that U_m^j becomes unbounded is almost zero; ii) using the expression $\bar{U} = \mathbb{E}[U_m^j]$, as defined in Subsection IV-A.

Corollary 1: *With the conditions in Lemma 1, we can further bound the one-step difference of F as*

$$\begin{aligned} \mathbb{E} [F(\mathbf{w}^{j+1}) - F(\mathbf{w}^j)] &\leq -\frac{(\bar{U} - 1 + \delta)\alpha}{2} \|\nabla F(\mathbf{w}^j)\|^2 \\ &+ \frac{L \alpha^2 U_0 C}{2B} \left(\frac{U_0}{S^j} + \frac{L(2U_0 - 1)(U_0 - 1)\alpha}{6} \right) \end{aligned} \quad (18)$$

given $U_m^j \leq U_0, \forall m, j$, for some constant U_0 .

Proof. The proof is provided in Appendix B. \square

From the second term of the RHS of (18), it can be inferred that a larger K tend to reduce the variance term since K is positively related with S^j . This implies that increasing the number of participating workers can speed up the training process round-wise. Building on Corollary 1, we are now ready to establish the main result.

Theorem 1: *Under the conditions in Lemma 1, the expectation of the average squared norm of the gradients can be upper bounded by*

$$\begin{aligned} \frac{1}{J} \mathbb{E} \left[\sum_{j=0}^{J-1} \|\nabla F(\mathbf{w}^j)\|^2 \right] &\leq \frac{2(F(\mathbf{w}^0) - F^*)}{(\bar{U} - 1 + \delta)\alpha J} \\ &+ \frac{L\alpha U_0 C}{(\bar{U} - 1 + \delta)B} \left(\frac{U_0}{K} + \frac{L(2U_0 - 1)(U_0 - 1)\alpha}{6} \right). \end{aligned} \quad (19)$$

Proof. The proof is presented in Appendix C. \square

Theorem 1 states that STSyn can achieve a sublinear convergence rate $\mathcal{O}(1/J)$, providing a theoretical guarantee for the performance of STSyn, which is consistent with the result of local SGD in i.i.d. data case [15]. Compared with the convergence upper bound in [15] where each uploading worker performs the same number of, i.e., U , local updates, here in (19) the role of U is replaced with \bar{U} and U_0 , which are the average and upper bound of U_m^j , respectively. Since \bar{U} is larger than U as discussed in Section IV-B, the first term of the RHS of (19) is smaller, and it is also conducive to reducing the variance term (the second term). Therefore, so long as the first term dominates (which is indeed the case for i.i.d. data distribution in our experimental setting, demonstrated by the results in the next section), a reduced upper bound than other local SGD schemes with the same number of local updates across workers is achieved. This thereby theoretically substantiates that the additional local updates can accelerate the training process round-wise with i.i.d. data.

V. EXPERIMENTS

In this section, we evaluate the effectiveness of the proposed STSyn. For comparison, we consider state-of-art schemes including AdaSync [37], PASGD [27] and AdaComm [28] mentioned in Subsection II-B. In addition, we explore the effect of the hyper-parameters K and U on the performance of STSyn.

A. Experimental Setting and Metric Calculation

Experimental Setting. We consider a two-layer fully connected neural network trained on the EMNIST dataset. All pieces of training data samples are shuffled and equally allocated to a sum of $M = 40$ workers. The mean of the exponential distribution of the computing time across workers is set to $\mu = 10^{-4}$ sec. The stepsize α is 0.1 and the batch size B is 100 for each scheme.

Metric Calculation. We determine the per-round metrics, i.e., wall-clock time and communication cost, for AdaSync, AdaComm and the proposed STSyn, as follows. Note that

we generally take one synchronous communication from the workers to the PS as one round.

Wall-clock time. At each fixed interval consisting of multiple rounds, with a deliberately chosen value K^j , AdaSync operates in an asynchronous manner by waiting for the fastest K workers in each round j . Hence, the wall-clock time consumed at round j can be expressed as

$$T_{AdaSync}^j \leq T_{K^j:M}^j. \quad (20)$$

For AdaComm, in each round j , each worker carries out τ^j local updates, with τ^j being decided adaptively. Then the per-round wall-clock time for AdaComm is

$$T_{AdaComm}^j = T_{M:M}^j, \quad (21)$$

Finally, as shown Section IV, the wall-clock time for STSyn at round j is given as

$$T_{STSyn}^j = T_{K:M}^j. \quad (22)$$

Communication cost. AdaSync is an asynchronous scheme, where the fastest K^j workers contribute to the update of the global parameter at the current round and the rest stragglers also make their contribution in following rounds. Therefore, the communication cost at round j can be regarded as the number of communication rounds between the K^j fastest workers and the PS, which is

$$C_{AdaSync}^j = 2K^j, \quad (23)$$

since in each round the fastest K^j workers download the global model from the PS and upload the gradient to the PS.

For AdaComm, the per-round communication cost is

$$C_{AdaComm}^j = 2M, \quad (24)$$

since the PS has to wait for all the workers in \mathcal{M} .

The communication cost for STSyn at round j is

$$C_{STSyn}^j = M + S^j, \quad (25)$$

since in STSyn all the workers in \mathcal{M} download the parameter \mathbf{w}^j from the PS but only the ones in the subset S^j upload their local parameters.

B. Experimental Results

STSyn Outperforms the State-of-the-Art Schemes.

Figs. 5 and 6 compare AdaSync, AdaComm, PASGD and STSyn in terms of test accuracy. Specifically, the initial number K_0 of workers to wait for in AdaSync is set to be 10; the initial number U_0 of local updates in AdaComm is set to be 20; the number of local updates U in PASGD is set to be 6, and STSyn is set with $K = 35$ and $U = 20$.

The performance of test accuracy against wall-clock time for the four schemes is shown in Fig. 5. It has to be pointed out that AdaSync exploits asynchronous mechanism by using stale gradients, which makes it a competitive scheme in terms of time efficiency. AdaComm is advantageous in runtime with local SGD by selecting the best communication frequency (i.e., U) in different time intervals. Despite all those, STSyn still enjoys the fastest training process thanks to the extra local updates and the robustness to stragglers while both AdaComm

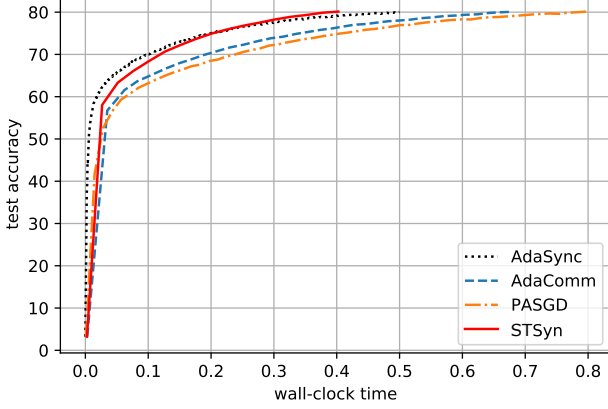


Fig. 5. Comparison of test accuracy against wall-clock time for AdaSync, AdaComm, PASGD and STSyn with $M = 40$.

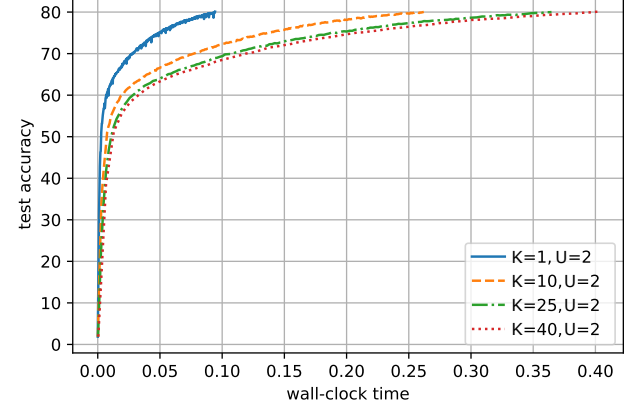


Fig. 7. Influence of hyper-parameter K of STSyn with $K = 1, 10, 25, 40$ in terms of time-to-accuracy performance.

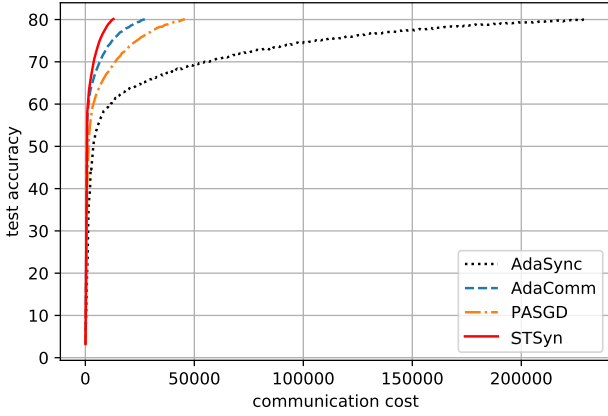


Fig. 6. Comparison of test accuracy versus communication cost for AdaSync, AdaComm, PASGD and STSyn with $M = 40$.

and PASGD are not straggler-tolerant. AdaComm performs better than PASGD due to its adaptive communication strategy. Although AdaSync outperforms the other three at the beginning, it indeed has the worst time efficiency mainly because of the staleness of the local gradients.

As illustrated in Fig. 6, STSyn also achieves the best communication-to-accuracy performance. With only part of the workers involved in the updates, the training speedup of STSyn in rounds can be comparable to AdaComm owing to the exploration of the additional effective local updates. This leads to a better communication efficiency for STSyn. PASGD has a larger communication cost than both STSyn and AdaComm due to the less utilization of local updates. Not surprisingly, AdaSync performs the worst since no local updates are performed.

Effect of Hyper-Parameter K . As discussed in Section IV, K affects the wall-clock time, the communication cost, as well as the number of local updates at each round. By comparing the STSyn schemes with different values of K and fixed U , we can observe the trade-off between wall-clock time

and communication cost from the perspective of accuracy.

In Fig. 7, the performances of test accuracy against wall-clock time for different values of K are illustrated. It can be seen that STSyn with a smaller K converges faster in the sense that the per-round runtime that the PS has to wait for is much reduced. It also implies that although more participating workers, as analyzed in Corollary 1, can reduce the variance of the aggregated model and thus speeding up the training process, waiting for fewer workers is more effective in improving the time efficiency of STSyn.

Fig. 8 illustrates the communication-to-accuracy performance of STSyn with different values of K . In stark contrast to the case of wall-clock time, it is shown that a larger K , implying a larger S^j , yields higher communication efficiency, which substantiates the analysis in (18) that more participating workers leads to larger variance reduction. This is because both the participating workers and local updates facilitate faster convergence in terms of training rounds, and the resulting speedup can compensate for the increase of per-round communication cost. As a result, there is a trade-off between communication cost and wall-clock time for STSyn.

Effect of Hyper-Parameter U . As analyzed in Section IV, U is positively related with the number of workers selected per round S^j ; hence, increasing U also means that more workers are selected each round.

In Fig. 9, the time-to-accuracy performance of STSyn with different values of U is illustrated. Similar to the case of K , the performance also decreases as U grows larger for a fixed value of K . This is because their influence on per-round wall-clock time, which is significantly raised to allow more local updates, is similar.

In Fig. 10, we plot the accuracy of STSyn in terms of communication cost with different values of U . It is shown that the communication efficiency is improved asymptotically as U grows larger and finally reaches a summit. The experiment results are consistent with the convergence analysis in (17). In particular, when U is relatively small, the communication efficiency also increases with U because the speedup brought by a larger U can compensate for the increased communication

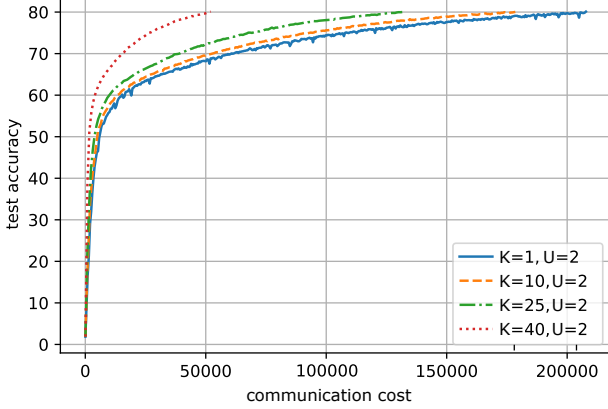


Fig. 8. Influence of hyper-parameter K of STSyn with $K = 1, 10, 25, 40$ in terms of communication-to-accuracy performance.

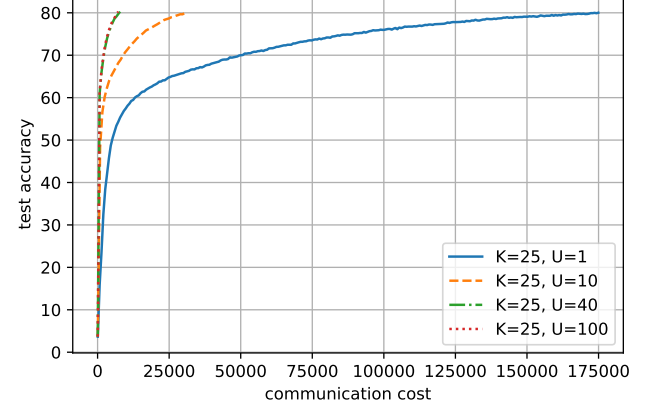


Fig. 10. Influence of hyper-parameter U of STSyn with $U = 1, 10, 40, 100$ in terms of communication-to-accuracy performance.

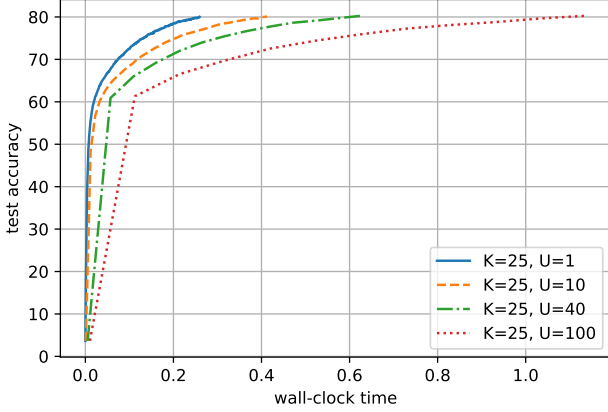


Fig. 9. Influence of hyper-parameter U of STSyn with $U = 1, 10, 40, 100$ in terms of time-to-accuracy performance.

cost. As U becomes relatively large, almost all the workers are able to finish at least one local update and hence can be selected; the resulted communication efficiency then stays still as U increases mainly because there is less room to improve the speedup. It also corroborates our analysis of Theorem 1 that the first term of the RHS of (19) to dominate for i.i.d. data case in this setting since we can hardly notice the influence of the increased variance caused by a larger U_0 in the figure.

To sum up, with respect to hyper-parameter K , the time efficiency of STSyn decreases while the communication efficiency decreases as K becomes larger. Hence, a value in the middle of $[1, M]$ is more desirable to achieve a balance. In regard to hyper-parameter U , the time efficiency also decreases but the communication efficiency stops increasing once U exceeds some threshold. Thus, we can choose U near the threshold value, which is 40 in this case, such that the best communication efficiency is achieved and a decent time efficiency is also attained.

VI. CONCLUSION

Building on a PS-based distributed learning framework, we proposed STSyn, a novel local-SGD scheme with heterogeneous synchronization, which is both straggler-tolerant and communication-efficient. We derived the average wall-clock time, average number of local updates and average number of uploading workers for the proposed STSyn to substantiate the effectiveness of the additional local updates. The convergence of STSyn under homogenous data distribution was also rigorously established. Extensive experimental results corroborated the superior time and communication efficiency of the proposed STSyn over the existing alternatives. The impacts of the hyper-parameters were also explored.

Our work leaves open a number of future research directions. First, it would be interesting to explore the potential advantages of heterogeneous synchronization for asynchronous implementations, where any worker can perform a number of local updates and send the result back to the PS. Second, generalization and analysis of the proposed STSyn scheme to the scenario where the wireless medium is considered, are worthy of further investigation. Lastly, integration of STSyn with the adaptive communication design might be also beneficial, and will be pursued in future work.

APPENDIX A PROOF OF LEMMA 1

Proof. The $(j+1)$ th global model parameter \mathbf{w}^{j+1} can be written as

$$\begin{aligned} \mathbf{w}^{j+1} &= \frac{1}{S^j} \sum_{m \in \mathcal{S}^j} \mathbf{w}_m^{j, U_m^j} \\ &= \frac{1}{S^j} \sum_{m \in \mathcal{S}^j} \left[\mathbf{w}_m^j - \sum_{u=0}^{U_m^j-1} \frac{\alpha}{B} \sum_{b=1}^B \nabla F(\mathbf{w}_m^{j,u}; \xi_{m,b}^{j,u}) \right], \end{aligned} \quad (26)$$

where $\xi_{m,b}^j$ is i.i.d. across all workers, iterations and mini-batch indices in i.i.d. data case.

According to (15) in Assumption 2, the one-step difference of the objective function can be written as

$$\begin{aligned}
& F(\mathbf{w}^{j+1}) - F(\mathbf{w}^j) \\
& \stackrel{(a)}{\leq} \langle \nabla F(\mathbf{w}^j), \mathbf{w}^{j+1} - \mathbf{w}^j \rangle + \frac{L}{2} \|\mathbf{w}^{j+1} - \mathbf{w}^j\|^2 \\
& \stackrel{(b)}{=} - \left\langle \nabla F(\mathbf{w}^j), \frac{\alpha}{S^j B} \sum_{m \in \mathcal{S}^j} \sum_{u=0}^{U_m^j-1} \sum_{b=1}^B \nabla F(\mathbf{w}_m^{j,u}; \xi_{m,b}^{j,u}) \right\rangle \\
& \quad + \frac{L}{2} \left\| \frac{\alpha}{S^j B} \sum_{m \in \mathcal{S}^j} \sum_{u=0}^{U_m^j-1} \sum_{b=1}^B \nabla F(\mathbf{w}_m^{j,u}; \xi_{m,b}^{j,u}) \right\|^2 \\
& \stackrel{(c)}{=} - \frac{\alpha}{S^j B} \sum_{m \in \mathcal{S}^j} \sum_{u=0}^{U_m^j-1} \sum_{b=1}^B \left\langle \nabla F(\mathbf{w}^j), \nabla F(\mathbf{w}_m^{j,u}; \xi_{m,b}^{j,u}) \right\rangle \\
& \quad + \frac{L\alpha^2}{2(S^j)^2 B^2} \left\| \sum_{m \in \mathcal{S}^j} \sum_{u=0}^{U_m^j-1} \sum_{b=1}^B \nabla F(\mathbf{w}_m^{j,u}; \xi_{m,b}^{j,u}) \right\|^2, \quad (27)
\end{aligned}$$

where (a) holds because of the boundedness in Assumption 2; (b) is due to (26); and (c) is obtained by interchanging the summation and the inner product.

Next, we will bound the expectation of the first and second term in (27), respectively. For the first term, we have

$$\begin{aligned}
& \mathbb{E} \left[-\frac{\alpha}{S^j B} \sum_{m \in \mathcal{S}^j} \sum_{u=0}^{U_m^j-1} \sum_{b=1}^B \left\langle \nabla F(\mathbf{w}^j), \nabla F(\mathbf{w}_m^{j,u}; \xi_{m,b}^{j,u}) \right\rangle \right] \\
& \stackrel{(a)}{=} -\frac{\alpha}{S^j} \sum_{m \in \mathcal{S}^j} \sum_{u=0}^{U_m^j-1} \mathbb{E} [\langle \nabla F(\mathbf{w}^j), \nabla F(\mathbf{w}_m^{j,u}) \rangle] \\
& \stackrel{(b)}{=} -\frac{\alpha}{2S^j} \sum_{m \in \mathcal{S}^j} \sum_{u=0}^{U_m^j-1} \left(\mathbb{E} [\|\nabla F(\mathbf{w}^j)\|^2] + \mathbb{E} [\|\nabla F(\mathbf{w}_m^{j,u})\|^2] \right) \\
& \quad + \frac{\alpha}{2S^j} \sum_{m \in \mathcal{S}^j} \sum_{u=0}^{U_m^j-1} \mathbb{E} [\|\nabla F(\mathbf{w}^j) - \nabla F(\mathbf{w}_m^{j,u})\|^2] \\
& \stackrel{(c)}{\leq} -\frac{\alpha}{2S^j} \sum_{m \in \mathcal{S}^j} \left[(U_m^j + 1) \|\nabla F(\mathbf{w}^j)\|^2 + \sum_{u=1}^{U_m^j-1} \mathbb{E} [\|\nabla F(\mathbf{w}_m^{j,u})\|^2] \right] \\
& \quad + \frac{L^2 \alpha}{2S^j} \sum_{m \in \mathcal{S}^j} \sum_{u=1}^{U_m^j-1} \mathbb{E} [\|\mathbf{w}^j - \mathbf{w}_m^{j,u}\|^2], \quad (28)
\end{aligned}$$

where (a) is due to the unbiasedness in Assumption 1; (b) simply rewrites the inner product; and (c) uses the fact that $\mathbf{w}_m^{j,0} = \mathbf{w}^j$ and the smoothness in Assumption 2. We now

proceed to bound the second term in (28), given as

$$\begin{aligned}
& \mathbb{E} [\|\mathbf{w}^j - \mathbf{w}_m^{j,u}\|^2] \\
& \stackrel{(a)}{=} \frac{\alpha^2}{B^2} \mathbb{E} \left[\left\| \sum_{t=0}^{u-1} \sum_{b=1}^B \nabla F(\mathbf{w}_m^{j,t}; \xi_{m,b}^{j,t}) \right\|^2 \right] \\
& \stackrel{(b)}{\leq} \frac{\alpha^2 u}{B^2} \mathbb{E} \left[\sum_{t=0}^{u-1} \left\| \sum_{b=1}^B \nabla F(\mathbf{w}_m^{j,t}; \xi_{m,b}^{j,t}) \right\|^2 \right] \\
& \stackrel{(c)}{=} \frac{\alpha^2 u}{B^2} \mathbb{E} \left[\sum_{t=0}^{u-1} \left\| \sum_{b=1}^B \left(\Delta_{m,b}^{j,t} + \nabla F(\mathbf{w}_m^{j,t}) \right) \right\|^2 \right] \\
& \stackrel{(d)}{=} \frac{\alpha^2 u}{B^2} \mathbb{E} \left[\sum_{t=0}^{u-1} \left\| \sum_{b=1}^B \Delta_{m,b}^{j,t} \right\|^2 \right] + \alpha^2 u \mathbb{E} \left[\sum_{t=0}^{u-1} \|\nabla F(\mathbf{w}_m^{j,t})\|^2 \right] \\
& \quad + \frac{\alpha^2 u}{B^2} 2 \mathbb{E} \left[\sum_{t=0}^{u-1} \mathbb{E}_\xi \left\langle \sum_{b=1}^B \Delta_{m,b}^{j,t}, B \nabla F(\mathbf{w}_m^{j,t}) \right\rangle \right] \\
& \stackrel{(e)}{=} \frac{\alpha^2 u}{B^2} \mathbb{E} \left[\sum_{t=0}^{u-1} \sum_{b=1}^B \|\Delta_{m,b}^{j,t}\|^2 \right] + \alpha^2 u \mathbb{E} \left[\sum_{t=0}^{u-1} \|\nabla F(\mathbf{w}_m^{j,t})\|^2 \right] \\
& \stackrel{(e)}{\leq} \frac{\alpha^2 u^2 C}{B} + \alpha^2 u \mathbb{E} \left[\sum_{t=0}^{u-1} \|\nabla F(\mathbf{w}_m^{j,t})\|^2 \right], \quad (29)
\end{aligned}$$

where (a) is due to (26); (b) holds by following Cauchy-Schwartz inequality; (c) holds because we have defined $\Delta_{m,b}^{j,t} = \nabla F(\mathbf{w}_m^{j,t}; \xi_{m,b}^{j,t}) - \nabla F(\mathbf{w}_m^{j,t})$; (d) uses the expansion $(a+b)^2 = a^2 + 2ab + b^2$; (e) holds because $\mathbb{E} [\|(\nabla F(\mathbf{w}_m^{j,t}; \xi_{m,b}^{j,t}) - \nabla F(\mathbf{w}_m^{j,t}))\|^2] = 0$ due to the unbiasedness of the stochastic gradient in Assumption 1, and hence we could use the fact that $\mathbb{E} [\|\sum_{i=1}^n X_i\|^2] = \sum_{i=1}^n \mathbb{E} [\|X_i\|^2]$ when $EX_1 = \dots = EX_n = 0$; and (f) holds because of the bounded variance of the stochastic gradient in Assumption 1.

By plugging (29) into (28) and through rearrangement, we can directly obtain

$$\begin{aligned}
& \mathbb{E} \left[-\frac{\alpha}{S^j B} \sum_{m \in \mathcal{S}^j} \sum_{u=0}^{U_m^j-1} \sum_{b=1}^B \left\langle \nabla F(\mathbf{w}^j), \nabla F(\mathbf{w}_m^{j,u}; \xi_{m,b}^{j,u}) \right\rangle \right] \\
& \leq -\frac{1}{S^j} \sum_{m \in \mathcal{S}^j} \frac{(U_m^j + 1)\alpha}{2} \left(1 - \theta_1^{m,j} \right) \|\nabla F(\mathbf{w}^j)\|^2 \\
& \quad - \frac{1}{S^j} \sum_{m \in \mathcal{S}^j} \left[\frac{\alpha}{2} \left(1 - \theta_2^{m,j} \right) \sum_{u=1}^{U_m^j-1} \mathbb{E} [\|\nabla F(\mathbf{w}_m^{j,u})\|^2] - \theta_3^{m,j} \right], \quad (30)
\end{aligned}$$

where we have defined $\theta_1^{m,j} = \frac{L^2 \alpha^2 U_m^j (U_m^j - 1)}{2(U_m^j + 1)}$, $\theta_2^{m,j} = \frac{L^2 \alpha^2 (U_m^j + 1)(U_m^j - 2)}{2}$, $\theta_3^{m,j} = \frac{L^2 \alpha^3 C (2U_m^j - 1) U_m^j (U_m^j - 1)}{12B}$.

Similar to (29), we can bound the second term of (27) as

follows:

$$\begin{aligned}
& \frac{L\alpha^2}{2(S^j)^2 B^2} \mathbb{E} \left[\left\| \sum_{m \in \mathcal{S}^j} \sum_{u=0}^{U_m^j-1} \sum_{b=1}^B \nabla F(\mathbf{w}_m^{j,u}; \xi_{m,b}^{j,u}) \right\|^2 \right] \\
& \stackrel{(a)}{\leq} \frac{L\alpha^2}{2S^j B^2} \mathbb{E} \left[\sum_{m \in \mathcal{S}^j} U_m^j \sum_{u=0}^{U_m^j-1} \left\| \sum_{b=1}^B \nabla F(\mathbf{w}_m^{j,u}; \xi_{m,b}^{j,u}) \right\|^2 \right] \\
& \stackrel{(b)}{=} \frac{L\alpha^2}{2S^j B^2} \mathbb{E} \left[\sum_{m \in \mathcal{S}^j} U_m^j \sum_{u=0}^{U_m^j-1} \left\| \sum_{b=1}^B \left(\Delta_{m,b}^{j,u} + \nabla F(\mathbf{w}_m^{j,u}) \right) \right\|^2 \right] \\
& \stackrel{(c)}{\leq} \frac{1}{S^j} \sum_{m \in \mathcal{S}^j} \left[\frac{L(U_m^j)^2 \alpha^2 C}{2B} + \frac{LU_m^j \alpha^2}{2} \sum_{u=0}^{U_m^j-1} \mathbb{E} \left[\left\| \nabla F(\mathbf{w}_m^{j,u}) \right\|^2 \right] \right], \tag{31}
\end{aligned}$$

where (a) is due to Cauchy-Schwartz inequality; (b) is direct from (a); and (c) is obtained the same way as in (29).

By summing up the upper bounds (30) and (31) for the two terms in (27), we have

$$\begin{aligned}
& \mathbb{E} [F(\mathbf{w}^{j+1}) - F(\mathbf{w}^j)] \\
& \stackrel{(a)}{\leq} \frac{1}{S^j} \sum_{m \in \mathcal{S}^j} -\frac{(U_m^j + 1)\alpha}{2} \left(1 - \theta_1^{m,j} - \frac{L\alpha U_m^j}{U_m^j + 1} \right) \left\| \nabla F(\mathbf{w}^j) \right\|^2 \\
& \quad - \frac{1}{S^j} \sum_{m \in \mathcal{S}^j} \frac{\alpha}{2} \left(1 - \theta_2^{m,j} - L\alpha U_m^j \right) \sum_{u=1}^{U_m^j-1} \mathbb{E} \left[\left\| \nabla F(\mathbf{w}_m^{j,u}) \right\|^2 \right] \\
& \quad + \frac{1}{S^j} \sum_{m \in \mathcal{S}^j} \theta_3^{m,j} + \frac{1}{S^j} \sum_{m \in \mathcal{S}^j} \frac{L(U_m^j)^2 \alpha^2 C}{2B} \\
& \stackrel{(b)}{\leq} \frac{1}{S^j} \sum_{m \in \mathcal{S}^j} -\frac{(U_m^j + 1)\alpha}{2} \left(1 - \theta_1^{m,j} - \frac{L\alpha U_m^j}{U_m^j + 1} \right) \left\| \nabla F(\mathbf{w}^j) \right\|^2 \\
& \quad + \frac{1}{S^j} \sum_{m \in \mathcal{S}^j} \theta_3^{m,j} + \frac{1}{S^j} \sum_{m \in \mathcal{S}^j} \frac{L(U_m^j)^2 \alpha^2 C}{2B} \\
& \stackrel{(c)}{\leq} \frac{1}{S^j} \sum_{m \in \mathcal{S}^j} -\frac{(U_m^j - L^2 \alpha^2)\alpha}{2} \left\| \nabla F(\mathbf{w}^j) \right\|^2 \\
& \quad + \frac{1}{S^j} \sum_{m \in \mathcal{S}^j} \theta_3^{m,j} + \frac{1}{S^j} \sum_{m \in \mathcal{S}^j} \frac{L(U_m^j)^2 \alpha^2 C}{2B} \\
& \stackrel{(d)}{\leq} -\frac{1}{S^j} \sum_{m \in \mathcal{S}^j} \frac{(U_m^j - 1 + \delta)\alpha}{2S} \left\| \nabla F(\mathbf{w}^j) \right\|^2 \\
& \quad + \frac{1}{S^j} \sum_{m \in \mathcal{S}^j} \frac{L\alpha^2 U_m^j C}{2B} \left(U_m^j + \frac{L(2U_m^j - 1)(U_m^j - 1)\alpha}{6} \right), \tag{32}
\end{aligned}$$

where (a) is due to rearrangement of terms; (b) is because of the condition $\theta_2^{m,j} + L\alpha U_m^j \leq 1$; (c) is also due to the above condition since it implies that $\frac{(U_m^j + 1)\alpha}{2S^j} \left(1 - \theta_1^{m,j} - \frac{L\alpha U_m^j}{U_m^j + 1} \right) \geq \frac{\alpha(U_m^j - L^2 \alpha^2)}{2S^j}$, which can be substantiated through direct computation; and (d) uses the condition $1 - \delta \geq L^2 \alpha^2$ for some $0 < \delta < 1$ and the combination of terms. The proof is now complete.

APPENDIX B PROOF OF COROLLARY 1

Proof. Revisiting (31), we have

$$\begin{aligned}
& \frac{L\alpha^2}{2(S^j)^2 B^2} \mathbb{E} \left[\left\| \sum_{m \in \mathcal{S}^j} \sum_{u=0}^{U_m^j-1} \sum_{b=1}^B \nabla F(\mathbf{w}_m^{j,u}; \xi_{m,b}^{j,u}) \right\|^2 \right] \\
& \leq \frac{LU_0 \alpha^2}{2(S^j)^2 B^2} \mathbb{E} \left[\sum_{u=0}^{U_0-1} \left\| \sum_{m \in \mathcal{S}^j} \sum_{b=1}^B \nabla F(\mathbf{w}_m^{j,u}; \xi_{m,b}^{j,u}) \right\|^2 \right] \\
& = \frac{LU_0^2 \alpha^2 C}{2(S^j)^2 B^2} \mathbb{E} \left[\sum_{u=0}^{U_0-1} \left\| \sum_{m \in \mathcal{S}^j} \sum_{b=1}^B \left(\Delta_{m,b}^{j,t} + \nabla F(\mathbf{w}_m^{j,u}) \right) \right\|^2 \right] \\
& \leq \frac{LU_0^2 \alpha^2 C}{2S^j B} + \frac{LU_0 \alpha^2}{2} \sum_{u=0}^{U_0} \mathbb{E} \left[\left\| \nabla F(\mathbf{w}_m^{j,u}) \right\|^2 \right]. \tag{33}
\end{aligned}$$

Combining (30) and (33) and the fact that $\frac{1}{S^j} \sum_{s \in \mathcal{S}^j} U_m^j = \bar{U}$, we can obtain Corollary 1 with the similar process in the proof of Lemma 1.

APPENDIX C PROOF OF THEOREM 1

Proof. By taking the summation on both sides of (18) from $j = 0$ to $J - 1$, we have

$$\begin{aligned}
& \mathbb{E} [F(\mathbf{w}^J) - F(\mathbf{w}^0)] \\
& \leq \sum_{j=0}^{J-1} -\frac{(\bar{U} - 1 + \delta)\alpha}{2} \left\| \nabla F(\mathbf{w}^j) \right\|^2 \\
& \quad + \sum_{j=0}^{J-1} \frac{L\alpha^2 U_0 C}{2B} \left(\frac{U_0}{S^j} + \frac{L(2U_0 - 1)(U_0 - 1)\alpha}{6} \right) \\
& \leq \sum_{j=0}^{J-1} -\frac{(\bar{U} - 1 + \delta)\alpha}{2} \left\| \nabla F(\mathbf{w}^j) \right\|^2 \\
& \quad + \frac{L\alpha^2 U_0 C J}{2B} \left(\frac{U_0}{K} + \frac{L(2U_0 - 1)(U_0 - 1)\alpha}{6} \right), \tag{34}
\end{aligned}$$

where the last inequality uses the fact that $S^j \geq K$. Rearranging (34), we have the expectation of the average squared norm of the gradient:

$$\begin{aligned}
\frac{1}{J} \mathbb{E} \left[\sum_{j=0}^{J-1} \left\| \nabla F(\mathbf{w}^j) \right\|^2 \right] & \leq \frac{2(F(\mathbf{w}^0) - F^*)}{(\bar{U} - 1 + \delta)\alpha J} \\
& \quad + \frac{L\alpha U_0 C}{(\bar{U} - 1 + \delta)B} \left(\frac{U_0}{K} + \frac{L(2U_0 - 1)(U_0 - 1)\alpha}{6} \right), \tag{35}
\end{aligned}$$

where we used Assumption 2, i.e., $F^* - F(\mathbf{w}^0) \leq F(\mathbf{w}^J) - F(\mathbf{w}^0)$. The proof is then complete.

REFERENCES

- [1] L. Bottou, "Large-scale machine learning with stochastic gradient descent," in *Proc. COMPSTAT*, 2010, pp. 177–186.
- [2] X. Lian, C. Zhang, H. Zhang, C. J. Hsieh, W. Zhang, and J. Liu, "Can decentralized algorithms outperform centralized algorithms? A case study for decentralized parallel stochastic gradient descent," in *Proc. Neural Inf. Process. Syst.*, vol. 30, 2017, pp. 5336–5346.

[3] Z. Jiang, A. Balu, C. Hegde, and S. Sarkar, "Collaborative deep learning in fixed topology networks," in *Proc. Neural Inf. Process. Syst.*, vol. 30, 2017, pp. 5906–5916.

[4] M. Li, D. G. Andersen, J. W. Park, A. J. Smola, and B. Y. Su, "Scaling distributed machine learning with the parameter server," in *Proc. USENIX Symp. Oper. Syst. Des. Implement.*, 2014, pp. 583–598.

[5] J. Dean, G. S. Corrado, R. Monga, C. Kai, and A. Y. Ng, "Large scale distributed deep networks," in *Proc. Neural Inf. Process. Syst.*, vol. 25, 2012, pp. 1223–1231.

[6] M. Zinkevich, M. Weimer, A. J. Smola, and L. Li, "Parallelized stochastic gradient descent," *Proc. Neural Inf. Process. Syst.*, vol. 23, pp. 2595–2603, 2010.

[7] F. Sattler, S. Wiedemann, K.-R. Müller, and W. Samek, "Robust and communication-efficient federated learning from Non-iid data," *IEEE Trans. Neural Netw. and Learn. Syst.*, vol. 31, no. 9, pp. 3400–3413, 2019.

[8] H. Cui, J. Cipar, Q. Ho, J. Kim, S. Lee, A. Kumar, J. Wei, D. Wei, G. R. Ganger, and P. B. Gibbons, "Exploiting bounded staleness to speed up big data analytics," in *Proc. USENIX Annu. Tech. Conf.*, 2014, pp. 37–48.

[9] S. Gupta, W. Zhang, and F. Wang, "Model accuracy and runtime tradeoff in distributed deep learning: A systematic study," in *Proc. IEEE Int. Conf. Data Mining*, 2016, pp. 171–180.

[10] P. Goyal, P. Dollár, R. Girshick, P. Noordhuis, L. Wesolowski, A. Kyrola, A. Tulloch, Y. Jia, and K. He, "Accurate, large minibatch SGD: Training imagenet in 1 hour," *arXiv preprint arXiv:1706.02677*, 2017.

[11] P. Dube, T. Suk, and C. Wang, "AI gauge: Runtime estimation for deep learning in the cloud," in *Proc. IEEE Int. Symp. Comput. Architecture and High Perform. Comput.*, 2019, pp. 160–167.

[12] V. Smith, C.-K. Chiang, M. Sanjabi, and A. Talwalkar, "Federated multi-task learning," in *Proc. Neural Inf. Process. Syst.*, vol. 30, 2017, pp. 4427–4437.

[13] Y. Arjevani and O. Shamir, "Communication complexity of distributed convex learning and optimization," in *Proc. Neural Inf. Process. Syst.*, vol. 28, 2015, pp. 1756–1764.

[14] H. B. McMahan, E. Moore, D. Ramage, S. Hampson, and B. A. Arcas, "Communication-efficient learning of deep networks from decentralized data," in *Proc. Artif. Intell. and Statist.*, 2017, pp. 1273–1282.

[15] F. Zhou and G. Cong, "On the convergence properties of a K-step averaging stochastic gradient descent algorithm for nonconvex optimization," in *Proc. Int. Joint Conf. Artif. Intell.*, 2018, pp. 3219–3227.

[16] S. U. Stich, "Local SGD converges fast and communicates little," in *Proc. Proc. Int. Conf. Learn. Representations*, 2019.

[17] J. Wang and G. Joshi, "Cooperative SGD: A unified framework for the design and analysis of communication-efficient SGD algorithms," in *Proc. ICML Workshop Coding Theory Mach. Learn.*, 2019.

[18] B. Woodworth, J. Wang, B. McMahan, and N. Srebro, "Graph oracle models, lower bounds, and gaps for parallel stochastic optimization," *Proc. Neural Inf. Process. Syst.*, vol. 31, pp. 8505–8515, 2018.

[19] X. Li, K. Huang, W. Yang, S. Wang, and Z. Zhang, "On the convergence of FedAvg on Non-IID data," in *Proc. Int. Conf. Learn. Representations*, 2019.

[20] A. Khaled, K. Mishchenko, and P. Richtárik, "First analysis of local GD on heterogeneous data," *arXiv preprint arXiv:1909.04715*, 2019.

[21] H. Yu, S. Yang, and S. Zhu, "Parallel restarted SGD with faster convergence and less communication: Demystifying why model averaging works for deep learning," in *Proc. AAAI Conf. Artif. Intell.*, vol. 33, no. 01, 2019, pp. 5693–5700.

[22] S. Wang, T. Tuor, T. Saloniidis, K. K. Leung, C. Makaya, T. He, and K. Chan, "Adaptive federated learning in resource constrained edge computing systems," *IEEE J. Sel. Areas Commun.*, vol. 37, no. 6, pp. 1205–1221, 2019.

[23] F. Haddadpour and M. Mahdavi, "On the convergence of local descent methods in federated learning," *arXiv preprint arXiv:1910.14425*, 2019.

[24] L. Tao, S. U. Stich, and M. Jaggi, "Don't use large mini-batches, use local SGD," in *Proc. Int. Conf. Learn. Representations*, 2019.

[25] J. Wang, Q. Liu, H. Liang, G. Joshi, and H. V. Poor, "Tackling the objective inconsistency problem in heterogeneous federated optimization," in *Proc. NeurIPS*, vol. 33, 2020, pp. 7611–7623.

[26] Y. Ruan, X. Zhang, S.-C. Liang, and C. Joe-Wong, "Towards flexible device participation in federated learning," in *Proc. Int. Conf. Artif. Intell. and Statist.*, 2021, pp. 3403–3411.

[27] F. Haddadpour, M. M. Kamani, M. Mahdavi, and V. R. Cadambe, "Local SGD with periodic averaging: Tighter analysis and adaptive synchronization," in *Proc. Neural Inf. Process. Syst.*, vol. 32, 2019, pp. 11 082–11 094.

[28] J. Wang and G. Joshi, "Adaptive communication strategies to achieve the best error-runtime trade-off in local-update SGD," in *Proc. Mach. Learn. and Syst.*, vol. 1, 2019, pp. 212–229.

[29] S. Shen, Y. Cheng, J. Liu, and L. Xu, "STL-SGD: Speeding up local SGD with stagewise communication period," in *Proc. AAAI Conf. Artif. Intell.*, vol. 35, no. 11, 2021, pp. 9576–9584.

[30] J. Dean and L. A. Barroso, "The tail at scale," *Commun. ACM*, vol. 56, no. 2, pp. 74–80, 2013.

[31] R. Tandon, L. Qi, A. G. Dimakis, and N. Karampatziakis, "Gradient coding: Avoiding stragglers in distributed learning," in *Proc. Int. Conf. Mach. Learn.*, 2017, pp. 3368–3376.

[32] S. Li, M. A. Maddah-Ali, Q. Yu, and A. S. Avestimehr, "A fundamental tradeoff between computation and communication in distributed computing," *IEEE Trans. Inf. Theory*, vol. 64, no. 1, pp. 109–128, 2017.

[33] H. Wang, Z. Charles, and D. Papailiopoulos, "Erasurehead: Distributed gradient descent without delays using approximate gradient coding," *arXiv preprint arXiv:1901.09671*, 2019.

[34] J. Zhang and O. Simeone, "Lagc: Lazily aggregated gradient coding for straggler-tolerant and communication-efficient distributed learning," *IEEE Trans. Neural Netw. and Learn. Syst.*, vol. 32, no. 3, pp. 962–974, 2020.

[35] E. Ozfatura, D. Gündüz, and S. Ulukus, "Gradient coding with clustering and multi-message communication," in *Proc. IEEE Data Sci. Workshop*, 2019, pp. 42–46.

[36] A. Harlap, H. Cui, W. Dai, J. Wei, G. R. Ganger, P. B. Gibbons, G. A. Gibson, and E. P. Xing, "Addressing the straggler problem for iterative convergent parallel ML," in *Proc. ACM Symp. Cloud Comput.*, 2016, pp. 98–111.

[37] S. Dutta, J. Wang, and G. Joshi, "Slow and stale gradients can win the race: Error-runtime trade-offs in distributed SGD," in *Proc. Int. Conf. Artif. Intell. and Statist.*, 2018, pp. 803–812.

[38] A. Agarwal and J. C. Duchi, "Distributed delayed stochastic optimization," in *Proc. Neural Inf. Process. Syst.*, vol. 24, 2011, pp. 873–881.

[39] F. Niu, B. Recht, C. Re, and S. J. Wright, "Hogwild!: A lock-free approach to parallelizing stochastic gradient descent," in *Proc. Neural Inf. Process. Syst.*, vol. 24, 2011, pp. 693–701.

[40] X. Pan, M. Lam, S. Tu, D. Papailiopoulos, C. Zhang, M. I. Jordan, K. Ramchandran, C. Re, and B. Recht, "Cyclades: Conflict-free asynchronous machine learning," in *Proc. Neural Inf. Process. Syst.*, vol. 29, 2016, pp. 2576–2584.

[41] X. Lian, Y. Huang, Y. Li, and J. Liu, "Asynchronous parallel stochastic gradient for nonconvex optimization," in *Proc. Neural Inf. Process. Syst.*, vol. 28, 2015, pp. 2737–2745.

[42] S. Sra, A. W. Yu, M. Li, and A. J. Smola, "Adadelay: Delay adaptive distributed stochastic optimization," in *Proc. Artif. Intell. and Statist.*, 2016, pp. 957–965.

[43] S. Zheng, Q. Meng, T. Wang, W. Chen, N. Yu, Z. M. Ma, and T. Y. Liu, "Asynchronous stochastic gradient descent with delay compensation," in *Proc. Int. Conf. Mach. Learn.*, 2017, pp. 4120–4129.

[44] S. Nadarajah, "Explicit expressions for moments of order statistics," *Statistics & Probability Letters*, vol. 78, no. 2, pp. 196–205, 2008.